

Complete Structure of Gauche 1,1,2,2-Tetrafluoroethane Determined by Microwave Spectroscopy

Belén Maté, Angela Hight Walker, and R. D. Suenram

Optical Technology Division, National Institute of Standards and Technology,
Gaithersburg, Maryland 20899-8441

Norman C. Craig*

Department of Chemistry, Oberlin College, Oberlin, Ohio 44074

Received: May 24, 2000; In Final Form: July 31, 2000

The complete molecular structure of the high-energy gauche rotamer of 1,1,2,2-tetrafluoroethane (TFEA), Freon F134, has been determined using pulsed-molecular-beam Fourier transform microwave spectroscopy. Five different ^{13}C - and ^2H -substituted isotopomers, in addition to the normal species, were studied. Unlike the nonpolar anti rotamer, the gauche form has a permanent electric dipole moment, which permits a direct rotational analysis. The electric dipole moment was also determined using the Stark effect of two low- J transitions. The resulting dipole moment is $\mu_c = 8.186(7) \times 10^{-30} \text{ C m}$ [2.454(2) Debye] where the numbers in parentheses are the standard uncertainties (i.e., 1σ). The experimental results for the geometric parameters of TFEA are compared with two recent ab initio calculations.

Introduction

Some small fluorocarbons have surprising energy relations between isomers and rotamers. *cis*-1,2-Difluoroethylene is 4.52 kJ/mol lower in energy than its trans isomer in the gas phase despite the closer proximity of substantial partial negative charges in the cis isomer.¹ The double bond is not required for this effect. The gauche rotamer of 1,2-difluoroethane is 2.4 to 3.4 kJ/mol lower in energy than the anti rotamer in the gas phase.^{2,3} These two striking outcomes are examples of what are known, respectively, as the cis effect and the gauche effect.

The seemingly anomalous energetics in molecules of interest here are encompassed, however, by high-level ab initio calculations. For example, with the formulation of the hybrid Hartree–Fock density functional theory known as the adiabatic connection method (ACM), *cis*-difluoroethylene is 2 kJ/mol lower in energy than its trans isomer, in fair agreement with experiment.⁴ Similarly, the energy of the gauche rotamer of difluoroethane is computed as 4.2 kJ/mol lower than the energy of the anti rotamer, also in fair agreement with experiment.

Several qualitative theories have been proposed to account for the preference for the cis or gauche form. Some theories attribute the preference for fluorine atoms to be adjacent to a favorable four-center interaction between CF bonds.⁵ Thus, a special interaction lowers the energy of the cis or gauche form. In contrast, Wiberg's bent bond theory attributes the effect to a destabilization of the trans or anti species.⁶ Thus, the σ part of the double bond is weakened because the carbon orbitals in the trans or anti form point on opposite sides of the direct line between the carbon atoms and thus have relatively poor overlap. By either line of reasoning, one predicts that 1,1,2,2-tetrafluoroethane (TFEA) should be an even more astounding example of the gauche effect. Yet, experiment and ACM calculations show that the anti rotamer has the lower energy in TFEA.⁴

Calculations by Papasavva et al. with an MP2/6-31G** model give similar results.⁷ The energy difference found by experiment is about 5 kJ/mol in favor of the anti rotamer in the gas phase;⁸ the energy difference found by calculation is 5.4 to 6.9 kJ/mol in favor of the anti rotamer.^{4,7} On the other hand, by valence bond arguments Epitotis has accounted for the different energy preferences between the difluoroethane rotamers and the tetrafluoroethane rotamers.⁹

Recent structural studies have shown that significant adjustments in bond lengths and bond angles occur in going between the two isomers of 1,2-difluoroethylene^{10,11} and in going between the two rotamers of 1,2-difluoroethane.^{12,13} Good structural information not only gives clues to the electronic adjustments but also gives a basis for evaluating ab initio calculations. Microwave spectroscopy has provided the structural information about the polar cis and gauche species. For the nonpolar trans and anti species, recent advances in recording and analyzing high-resolution infrared spectra have made feasible determining the structures of such species. The present paper is part of a comparable investigation of the complete structures of the two rotamers of TFEA. This part is concerned with the structure of the polar gauche rotamer as determined by microwave spectroscopy. A parallel investigation of the structure of the nonpolar anti rotamer is being carried out by high-resolution infrared spectroscopy.

Stone et al. did a preliminary structural investigation of the two rotamers of TFEA.¹⁴ Their microwave investigation gave good rotational constants for the normal species of the gauche rotamer and tentative rotational constants for the singly substituted ^{13}C species in natural abundance. Using electron diffraction results¹⁵ as well as the rotational constants from the microwave study, they proposed a partial structure for this rotamer. They also investigated the high-resolution infrared spectrum of the anti rotamer in a jet-cooled beam. This analysis yielded rotational constants for the anti rotamer. With no isotopic data

* To whom correspondence should be addressed.

for the anti rotamer, they transferred all of the structural parameters, except the CC bond length, for the gauche rotamer to the anti rotamer and fit the CC bond length of the anti rotamer. Such limited data provided no basis for comparing the structures of the two rotamers.

To obtain complete structures of the two rotamers of TFEA, isotopic species in addition to the normal and the $^{13}\text{C}_1$ species were needed. A deuterium-substituted species was essential to determine the position of the hydrogen atoms. The dideutero species and the $^{13}\text{C}_2$ species were synthesized. Additional isotopic species were desirable to provide a sufficient set of rotational constants for use in refining the coordinates of the fluorine atoms, which cannot be substituted. Accompanying the dideutero species were the d_1 and $^{13}\text{C}-d_2$ variants in observable amounts.

Experimental Section

Syntheses. The d_2 and $^{13}\text{C}_2$ isotopomers were prepared by an adaptation of the chemistry used to make isotopomers of 1,2-difluoroethane.¹³ Tetrabromoethane (TBrEA) was converted into TFEA by the action of AgF_2 at 150 °C. The high temperature is needed to convert the intermediate 1,1-dibromo-2,2-difluoroethane into the final product. As the starting material for TFEA- d_2 and TFEA- $^{13}\text{C}_2$, the corresponding TBrEAs were prepared from commercially available acetylene- d_2 and acetylene- $^{13}\text{C}_2$ by reaction with Br_2 . Details of the preparation and characterization of tetrafluoroethane- $^{13}\text{C}_2$ and - d_2 are given elsewhere.¹⁶

Fourier Transform Microwave (FTMW) Spectrometer.

The rotational spectra were studied using the FTMW spectrometers at National Institute of Standards and Technology (NIST). The current configuration is described in Suenram et al.¹⁷ Briefly, in this type of experiment, the sample gas of interest is in a dilute mixture with an inert carrier gas and pulsed through a commercial valve into a Fabry–Perot cavity, which is housed in a diffusion-pumped vacuum chamber. The pulsed valve is attached to the rear of one of the cavity mirrors and injects the gas through a 1-mm hole in the mirror. In all the experiments except the Stark experiments (described in a later section), the gas is injected along the Fabry–Perot cavity axis. The expansion process adiabatically cools the molecules in the gas to near 1 K. Once the gas pulse is in the center of the Fabry–Perot cavity, a microwave pulse of short duration (1 to 2 μs) is sent into the cavity to energize the molecules. If the gas of interest has a rotational transition within the cavity bandwidth [~ 500 kHz (full width at half-maximum)], the Fourier components of the microwave pulse pump the rotational transition. After the microwave pulse is discontinued and the cavity ringing has ceased (5 to 15 μs), the molecular emission in the cavity is digitized for 512 μs (4096 points at 125 ns/point). This signal is then Fourier transformed and displayed on a computer screen. The entire process is repeated at a 10-Hz repetition rate until an adequate signal-to-noise ratio is attained.

Because relatively small samples were available for the various isotopomers, dilute sample mixtures were used. All samples were prepared using an 80% Ne, 20% He spark chamber mixture as the carrier gas. Initial spectral predictions for the various isotopomers were made from reported structural parameters.¹⁴ The predictions were then adjusted using the differences between the observed and calculated rotational constants of the normal species. Relatively short, automated survey scans of 100 to 200 MHz were used to locate the transitions of interest for the various isotopic species.

Sample Descriptions. TFEA- $^{13}\text{C}_1$. Because the gauche rotamer of TFEA lies 5 kJ/mol in energy above the anti rotamer,

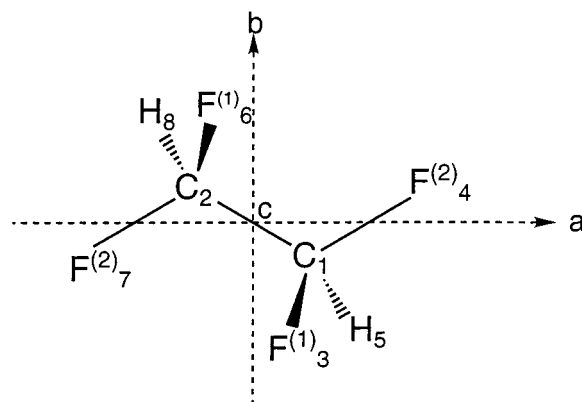


Figure 1. A sketch of the gauche rotamer that shows the approximate locations of the principal axes. The center of mass lies above the almost planar $\text{F}_7\text{C}_2\text{C}_1\text{F}_4$ sequence, and the c axis is coincident with the C_2 symmetry axis.

this rotamer is of low abundance and its spectra are of low intensity. The TFEA- $^{13}\text{C}_1$ isotopomer was observed in natural abundance using a 0.5% mixture of TFEA in the carrier gas. On the basis of this mixing ratio, the concentration of the $^{13}\text{C}_1$ isotopomer was 100 $\mu\text{mol/mol}$ of carrier gas.

The observation of the $^{13}\text{C}_1$ isotopomer served as a reference for the concentrations of the other rare isotopomers that were used. At this concentration the stronger transitions could be observed using the co-added signals from 10 nozzle pulses. The transition line widths for TFEA are also larger than normally observed. This broadening is due to the unresolved nuclear spin interactions of the fluorine atoms. Line widths for the deuterated isotopomers were even larger because of the unresolved deuterium quadrupole splittings. Estimated standard uncertainties (1σ) in the frequency measurements are 6 and 10 kHz for the undeuterated and deuterated isotopomers, respectively.

TFEA- $^{13}\text{C}_2$. A 0.25 mmol (97 Pa [0.73 Torr]) sample of TFEA- d_2 was used in the preparation of the gas mixture. A total of 1.06 mol of carrier gas gave a total pressure of 0.53 MPa [3950 Torr]. The concentration of $^{13}\text{C}_2$ was approximately 180 $\mu\text{mol/mol}$ of carrier gas, which is about a factor of 2 larger than the mixture of the $^{13}\text{C}_1$ isotopomer described above.

TFEA- d_2 , TFEA- $^{13}\text{C}_1-d_1$, and TFEA- d_1 . A 1-mmol sample of TFEA- d_2 was used and diluted with 1.06 mol of carrier gas. The resulting mixture was approximately 940 $\mu\text{mol/mol}$ of carrier gas. The $^{13}\text{C}-d_2$ species was observed in natural abundance in the d_2 sample. Transitions from the $^{13}\text{C}-d_2$ were only a factor of 50 weaker than the d_2 transitions. In this sample, transitions from the d_1 isotopomer were also observed. This species was present because of incomplete deuteration during the synthesis.

Dipole Moment. The electric dipole moment was determined by studying the frequency shift of the $|M| = 0$ and 1 Stark transitions with applied electric field for the $2_{11} - 1_{01}$ and the $2_{20} - 1_{10}$ transitions. During these measurements, the zero field frequencies of these two transitions were remeasured and found to be at 13766.4639 and 18296.7012 MHz, respectively. These values differed by 6 and 5 kHz, respectively, from the values reported by Stone et al.¹⁴ The values reported here are believed to be more accurate than those reported previously, although the two values are within the reported standard deviations. For the dipole moment determinations, the pulsed nozzle was located to inject the gas sample perpendicular to the axis of the Fabry–Perot cavity. The orientation of the Stark plates with respect to the L-shaped microwave antennas provided $\Delta M = 0$ selection rules. A diagram of the experimental arrangement is shown in

TABLE 1: Measured Transition Frequencies^a for Five Isotopomers of Gauche 1,1,2,2-Tetrafluoroethane

$J'(K'_a K'_c) - J''(K''_a K''_c)$	¹³ CF ₂ H-CF ₂ H	O-C ^b	¹³ CF ₂ H- ¹³ CF ₂ H	O-C	CF ₂ D-CF ₂ D	O-C	¹³ CF ₂ D-CF ₂ D	O-C	CF ₂ H-CF ₂ D	O-C
1(1,0) - 0(0,0)					7762.5020	-7.9				
2(0,2) - 1(1,0)					7896.8870	2.6				
3(2,1) - 3(1,3)					8222.7230	8.4				
4(2,2) - 4(1,4)					9148.1770	-6.6				
5(3,3) - 5(2,3)					11192.1760	-1.2				
4(3,2) - 4(2,2)					11565.0160	-0.4				
3(0,3) - 2(1,1)	12735.2949	0.8			12702.9630	7.4	12663.7949	-0.7	12737.2393	-0.2
3(3,1) - 3(2,1)	12755.0449	-2.7								
4(3,1) - 4(2,3)	13010.0508	0.7	12984.3320	0.0						
2(1,1) - 1(0,1)	13724.2842	0.3	13681.9824	1.1	13299.0670	-6.4	13261.3262	-4.1	13530.9668	1.1
4(1,3) - 3(2,1)			14907.0820	0.7	15084.2540	-1.9				
5(1,5) - 4(2,3)	16215.1855	-0.2								
4(0,4) - 3(1,2)	17277.8145	-2.3	17229.4580	-1.7	17210.8590	-6.5	17162.6973	0.3	17261.9023	0.3
5(4,2) - 5(3,2)	17925.3730	0.5								
6(4,3) - 6(3,3)			17772.7852	0.2						
4(4,1) - 4(3,1)			17952.5742	-1.3						
4(4,0) - 4(3,2)			17965.8730	1.2						
2(2,0) - 1(1,0)	18249.3818	1.2	18202.3027	1.0	17473.5710	1.0	17434.3975	-3.0	17874.1738	1.2
2(2,1) - 1(1,1)	18549.6494	3.6	18500.3701	0.3	17750.9000	-4.1	17709.8789	3.3	18165.1641	-1.5
3(1,2) - 2(0,2)	19557.0479	-1.5	19493.8730	-0.9	18999.1390	-0.8	18942.1104	5.2	19309.6475	-1.1
5(0,5) - 4(1,3)	21440.5156	0.1	21386.8574	1.3						
3(2,1) - 2(1,1)	23366.6738	-0.5	23303.7383	0.1	22512.8450	2.4	22458.6211	1.7	22959.8096	-1.6
3(2,2) - 2(1,2)	24205.3926	-1.1	24136.7119	-0.9	23287.4440	5.0	23228.3906	-2.1	23772.0430	2.0
6(0,6) - 5(1,4)			25145.7207	-0.3	25153.4040	0.1				
4(1,3) - 3(0,3)	25600.7900	-0.8	25514.8506	-0.1	24894.1460	3.2	24816.1719	-1.6		

^a Transition frequencies are given in MHz. The estimated uncertainties in the frequency measurements are 6 and 10 kHz for the undeuterated and deuterated species respectively. See text for discussion of how the uncertainties were estimated. ^b The numbers in the O-C columns are the observed - calculated values from the centrifugal distortion fit.

TABLE 2: Spectroscopic Constants^a for Isotopic Forms of Gauche 1,1,2,2-Tetrafluoroethane

constants	¹³ C	¹³ C ₂	<i>d</i> ₂	¹³ C- <i>d</i> ₂	<i>d</i>
A/MHz	5240.5895(5)	5227.3986(3)	4994.211(2)	4983.509(6)	5120.591(4)
B/MHz	2827.9463(7)	2818.2427(4)	2768.329(2)	2759.317(2)	2803.507(1)
C/MHz	2495.6245(7)	2488.5640(6)	2461.351(2)	2454.590(1)	2481.123(1)
δ _J /kHz	0.495(6)	0.477(4)	0.41(2)	0.492 ^b	0.492 ^b
δ _K /kHz	14.4(3)	14.9(2)	12.4(8)	14.49 ^b	14.49 ^b
Δ _{JK} /kHz	-2.90(9)	-2.99(3)	-2.7(2)	-3.5(3)	-3.1(2)
Δ _J /kHz	1.70(1)	1.676(9)	1.50(3)	1.49(5)	1.68(4)
Δ _K /kHz	3.2(1)	3.29(5)	2.9(4)	-2.2(14)	6.5(8)
rms/kHz	2.2	1.3	6.5	5.0	2.5
n trans	15	15	17	9	8

^a Type A expanded uncertainties are given with a coverage factor $k = 2$, i.e., 2σ . ^b Set to the value of the normal species.

Figure 1 of Suenram et al.¹⁸ The two sheet metal Stark plates (25 × 25 cm) are spaced by approximately 26 cm and are attached to the rods that are used to mount the Fabry-Perot mirrors. They are electrically isolated from the rods via Teflon spacers.¹⁹ A commercial high-voltage power supply (FuG model HCD 14M 20 000)¹⁹ that delivers symmetric dual outputs permits one plate to be energized (-) with respect to ground and the other to be energized (+) with respect to ground. The effective plate spacing was calibrated using the $J = 1 - 0$ rotational transition of OCS at 12162.9785 MHz. The accepted value for the dipole moment of OCS is $2.3856(10) \times 10^{-30}$ C m [0.71519(3) Debye].²⁰

Calculations. Fitting to Watson-type rotational Hamiltonians was done with versions of Dr. Arthur Maki's ASYM program. Structure fitting was done with spread sheets for the Kraitchman substitution method and with Professor Richard Schwendeman's program, as modified at the University of Michigan and known as STRFIT87.

Results and Discussion

Tetrafluoroethane is a mixture of gauche and anti rotamers. Only the polar gauche rotamer has a microwave spectrum. The lower-energy anti rotamer is about 75% of the mixture in the

gas phase at room temperature and is increasingly favored as the temperature is lowered.¹⁶ Fortunately, a relatively high barrier of about 13 kJ/mol exists for conversion of the gauche rotamer into the anti rotamer.⁴ Consequently, vibrational relaxation is incomplete in the jet-cooled beam of the microwave experiment as the higher-energy rotamer gets trapped within its individual well.^{21,22} Thus, the gauche rotamer is observable in these low-temperature experiments.

As shown in Figure 1, the gauche rotamer has C_2 symmetry. The twofold symmetry axis is also the *c*-principal axis and the dipole axis. Thus, *c*-type selection rules apply for microwave transitions. The molecule is a rather asymmetric top with $\kappa = -0.756$ for the normal species. From Stark-effect measurements the dipole moment was found to be $8.186(7) \times 10^{-30}$ C m [2.454(2) Debye]. For comparison, Papisavva et al. computed 2.79 D for the dipole moment.⁷ Mukhtarov and Kuliev reported a dipole moment of 2.9 D from a microwave study of TFEA.²³ However, because none of the microwave transitions for TFEA observed by Stone et al.¹⁴ is in the extensive table of transitions in the Mukhtarov and Kuliev report, we suspect that their sample was not TFEA. The large discrepancy between the reported dipole moment and the present one is further reason to suspect their sample purity.

TABLE 3: Cartesian Coordinates for Gauche 1,1,2,2-Tetrafluoroethane in Principal Axis System (in Å)^a

	atom	<i>a</i>	<i>b</i>	<i>c</i>
C ₁	single subst. ^b	0.6826	-0.3200	-0.3801
	double subst. ^b	0.6826	-0.3200	-0.3801
C ₂	single subst. ^b	-0.6826	0.3200	-0.3801
	double subst. ^b	-0.6826	0.3199	-0.3801
H ₅	single subst. ^b	0.8299	-0.9963	-1.2406
	double subst. ^b	0.8298	-0.9970	-1.2402
H ₈	single subst. ^b	-0.8299	0.9963	-1.2406
	double subst. ^b	-0.8298	0.9969	-1.2402
F ₃ (1) ^c		0.8660	-1.0179	0.7581
F ₄ (2) ^c		1.6292	0.6527	-0.4522
F ₆ (1) ^c		-0.8660	1.0179	0.7581
F ₇ (2) ^c		-1.6292	-0.6527	-0.4522

^a The values of the atomic coordinates are given to the nearest 0.0001 Å to show the close agreement between the two different methods of determining the coordinates. The estimates of the uncertainties are generally best expressed by the Costain uncertainties, which are defined as 0.0015/|coordinate|. See text for a complete discussion of uncertainties. ^b Single- and double-substitution r_s values. ^c From mixed r_s/r_0 structure fitting.

In addition to the previous microwave study of the normal species,¹⁴ five isotopic species have been investigated. Observed microwave transitions for the five new species are shown in Table 1. A sufficient number of lines was identified and measured for the ¹³C₂, ¹³C₁, and *d*₂ species to permit fitting a full set of centrifugal distortion constants in Watson-type Hamiltonians, as had been done for the normal species. Although five lines for the ¹³C₁ species were reported before,¹⁴ additional lines were measured and included in the fit in the present study. The rotational constants are given in Table 2. The more extensive data set now available for the ¹³C₁ isotopomer gives significantly different rotational constants for this species. For the ¹³C₁, ¹³C₂ and *d*₂ species and the parent, satisfactory agreement exists between the centrifugal distortion constants.

For two of the isotopic species, ¹³C₁-*d*₂ and *d*₁, which were present in very low concentration in the samples available, the number of observed lines was insufficient to fit a full set of centrifugal distortion constants. The observed lines for these two species are given in Table 1. For both of these isotopomers, δ_J and δ_K were transferred from the Hamiltonian of the normal species, and the other three centrifugal distortion constants were refined along with *A*, *B*, and *C*. As seen in Table 2, the three Δ constants for the *d*₁ species are in reasonable accord with those for the isotopomers that were fit without constraints. For the ¹³C₂-*d*₂ species the result is less satisfactory. As seen in Table 2, the Δ_K constant is negative even though the other two Δ constants are reasonable. Trial fits omitting each of the nine observed lines for ¹³C₁-*d*₂ from the fitting gave no improvement.

Structure Fitting. As seen in Figure 1, the gauche rotamer of TFEA has two types of fluorine atoms. As a consequence,

its structure is a 10-parameter problem. Cartesian coordinates of the carbon and hydrogen atoms in the principal axis system of the parent molecule are readily calculated by the substitution method from the rotational constants of the normal species and the species in which ¹³C and *d*₁ have been substituted.²⁴ Excellent agreement was found between the substitution coordinates for the carbon and hydrogen atoms found from single substitution and from double substitution. This comparison is shown in Table 3. The largest difference is 0.0007 Å.

Because the fluorine atoms cannot be substituted with stable isotopes, finding the coordinates for the two types of fluorine atoms depends on having an excess of rotational constants for various isotopomers. Two methods were used to find the fluorine coordinates. In one method, the carbon and hydrogen coordinates were held at the values found from single substitution, and the fluorine coordinates were fitted to the full set of 18 observed rotational constants. In addition, to avoid a linear dependence in the coordinate fitting, the FCF angle was constrained to 108.7°, the value computed by Muir and Baker with the ACM method.⁴ The result is a set of mixed r_s/r_0 coordinates. An equivalent result was obtained when the rotational constants of the *d*₁ and ¹³C₁ species were omitted from the fitting in which the r_s Cartesian coordinates were used for the carbon and hydrogen atoms. The Cartesian coordinates resulting from r_s/r_0 analysis are given in Table 3. In the other method, all of the coordinates, with the exception of the constraint on the FCF angle, were fitted simultaneously to the 18 rotational constants to give an r_0 set of coordinates. In both calculations all the appropriate symmetry constraints were used. In addition, both fittings were repeated without constraining the FCF bond angle. Although both fittings in the absence of the FCF angle constraint had a linear dependence and thus large calculated uncertainties in the Cartesian coordinates, the computed Cartesian coordinates and the FCF angle were remarkably close to those obtained with the FCF angle constraint.

Geometric parameters for the bond lengths and bond angles were computed from the Cartesian coordinates. Table 4 gives the geometric parameters. Included are the parameters derived from both the r_s/r_0 and r_0 coordinate sets when the FCF angle was constrained to 108.7°. The parameters for the CC and CH bonds are identical in the two treatments, as could be anticipated from the extensive information regarding substitution of the carbon and hydrogen atoms. Because the outcome of these two methods is also quite close for the CF parameters, we have confidence in the result. Table 4 also has the geometric parameters derived from the r_0 calculation without imposing the constraint on the FCF angle. Because this fitting has a linear dependence, we cannot depend on it. However, the agreement with the result obtained with the FCF angle constraint is striking and reassuring. From this latter calculation the fitted FCF angle

TABLE 4: Geometric Parameters for Gauche 1,1,2,2-Tetrafluoroethane^a

	r_{CH}	r_{CC}	$r_{CF(1)}$	$r_{CF(2)}$	α_{CCH}	$\alpha_{CCF(1)}$	$\alpha_{CCF(2)}$	α_{FCF}	τ_{HCCH}	$\tau_{HCCF(1)}$	$\tau_{HCCF(2)}$
present work											
constr. r_s/r_0 ^b	1.104(4)	1.508(4)	1.348(5)	1.359(4)	112.4(3)	110.1(3)	109.1(4)	108.7	65.2(7)	173.4(68)	54.2(7)
constr. r_0 ^c	1.104	1.508	1.347	1.360	112.4	110.1	109.0	108.7	65.2	173.3	54.2
unconstr. r_0 ^d	1.104	1.508	1.347	1.359	112.4	109.9	109.2	108.8	65.2	173.5	54.2
M and B calc. ^e	1.092	1.528	1.348	1.357	110.0	110.5	108.6	108.7	67.4		
PI and K calc. ^f	1.089	1.515	1.359	1.365	112.0	109.2	108.1	109.0		173.2	
electr. diffr. ^g	1.098(6)	1.518(5)	1.350(2)	1.350(2)	110.3(10)	108.2(3)	108.2(3)	107.3(3)	78(2)		

^a Bond lengths in Å; bond angles in degrees. ^b The C and H Cartesian coordinates were constrained to the r_s values, and α_{FCF} was constrained to the calculated value of Muir and Baker. Costain uncertainties in parentheses. The Costain uncertainties in the bond lengths and angles are propagated from the uncertainties in the atomic coordinates and are defined as 0.0015/(value of the atomic coordinate). See text for a detailed discussion of the uncertainties associated with the bond and angle parameters. ^c α_{FCF} was constrained. ^d Unconstrained. ^e Muir and Baker, ref 4. ^f Papasavva et al. ref 7. ^g Brown and Beagley, ref 15.

is 108.8°, which is very close to the angle of 108.7° used in the constraint. Associated with the r_s/r_0 geometric parameters in Table 4 are Costain uncertainties in parentheses. The Costain uncertainties in the bond lengths and angles are propagated from the uncertainties in the atomic coordinates and are defined as $0.0015/(\text{value of the atomic coordinate})$. These uncertainties are not given for the other two fittings because they are essentially the same as for the r_s/r_0 set. All of the Costain uncertainties are satisfactory except for the HCCF⁽¹⁾ torsional angle for which the uncertainty is 6.8°.

A further exploration of the fitting was done by varying the constrained FCF angle by $\pm 0.5^\circ$. The differences in CF bond lengths fell within the Costain uncertainties. The differences in the two CCF bond angles were 0.6° to 0.7° and thus somewhat larger than the Costain uncertainties. The differences in the torsional angles were covered by the Costain uncertainties.

Table 4 gives a comparison of the geometric parameters found by this microwave study with those found by ab initio calculations and by electron diffraction. Of course, exact agreement between the various methodologies is not to be expected because they explore the molecule in different ways. Two previously published ab initio calculations give geometric parameters for the rotamers of TFEA. One is the work of Muir and Baker, who used the ACM, which is a hybrid Hartree–Fock density functional method.⁴ The other is the work of Papasavva et al., who used an MP2/6-31G** model.⁷ The results of these two ab initio treatments are included in Table 4 for comparison with the new microwave results. The results of both ab initio calculations compare favorably with the observed values. With the exception of the r_{CC} and α_{CCH} , however, the results of the ACM are closer to the observed values than are the results of the MP2 calculations. Also included in Table 4 are the earlier electron diffraction results of Brown and Beagley.¹⁵ They reported average parameters for the two rotamers obtained from experiments at -20°C , where the gauche rotamer is only about 15% of the mixture. Not only did they have difficulty distinguishing the contribution of the unfavored gauche rotamer in the mixture, but they had to use an incomplete and a partly incorrect assignment of vibrational fundamentals¹⁶ in constructing a force field for estimating the effect of atomic displacements on the electron diffraction data. Thus, we do not regard these electron diffraction results as a useful comparison with the results of the microwave investigation even though they are reasonably close in most cases.

Reaching the principal goal of comparing the structure of the gauche rotamer of TFEA with the structure of its anti rotamer must await completion of our parallel investigation of the nonpolar anti rotamer by high-resolution infrared spectroscopy. Reaching that goal is in sight. Rotational constants for the parent of the anti species were reported in the previous study,¹⁴ and those results have been extended and reinforced by our analysis of the rotational structure due to the anti rotamer in the high-resolution infrared spectrum of TFEA. In addition, the analysis of the corresponding rotational structure in the spectrum of the d_2 species has been completed. The analysis of the spectrum of the $^{13}\text{C}_2$ species is nearing completion.

Summary. Five deuterium and carbon-13 isotopic modifications of the gauche rotamer of TFEA have been investigated by microwave spectroscopy in the 7 to 26 GHz region. A

Watson-type Hamiltonian with centrifugal distortion constants has been fitted to the observed transitions for each species. These new results supplement the previous investigation of the parent and a partial study of the $^{13}\text{C}_1$ species.¹⁴ For the gauche rotamer, which has only C_2 symmetry and two types of fluorine atoms, Cartesian coordinates have been found, and the 10 different bond and angle parameters have been determined. A dipole moment of $\mu_c = 8.186(7) \times 10^{-30}$ C m [2.454(2) Debye] has been found from the analysis of a Stark experiment. Two previous ab initio calculations, one using the hybrid Hartree–Fock density functional method (ACM)⁴ and the other an MP2/6-31G** model,⁷ are in reasonable agreement with the experimental findings.

Acknowledgment. The work on this project at Oberlin College was supported by the National Science Foundation with grant CHE 9710375 and Oberlin College. We are grateful for the contributions of Jessica I. Chuang, Christiana C. Nwofor, and Catherine M. Oertel, who did the syntheses of the isotopic species.

References and Notes

- (1) Craig, N. C.; Brandon, D. W.; Stone, S. C.; Lafferty, W. J. *J. Phys. Chem.* **1992**, *96*, 1598.
- (2) Huber-Wälchli, P.; Günthard, H. *Spectrochim. Acta* **1981**, *37A*, 285.
- (3) Durig, J. R.; Liu, J.; Little, T. S.; Kalasinsky, V. F. *J. Phys. Chem.* **1992**, *96*, 8224.
- (4) Muir, M.; Baker, J. *Mol. Phys.* **1996**, *89*, 211.
- (5) Engkvist, O.; Karlström, G.; Widmark, P.-O. *Chem. Phys. Lett.* **1997**, *265*, 19.
- (6) Wiberg, K. *Acc. Chem. Res.* **1996**, *29*, 229.
- (7) Papasavva, S.; Illinger, K. H.; Kenny, J. E. *J. Phys. Chem.* **1996**, *100*, 10100.
- (8) Kalasinsky, V. F.; Anjaria, H. V.; Little, T. S. *J. Phys. Chem.* **1982**, *86*, 1351.
- (9) Epiotis, N. D. *Deciphering the Chemical Code. Bonding Across the Periodic Table*; VCH Publishers: New York, 1996; Chapter 11.
- (10) Harmony, M. D.; Laurie, V. W.; Kuzckowski, R. L.; Schwendeman, R. H.; Ramsay, D. A.; Lovas, F. J.; Lafferty, W. J.; Maki, A. G. *J. Phys. Chem. Ref. Data* **1979**, *8*, 619.
- (11) Craig, N. C.; Abiog, O. P.; Hu, B.; Stone, S. C.; Lafferty, W. J.; Xu, L.-H. *J. Phys. Chem.* **1996**, *100*, 5310.
- (12) Takeo, H.; Matsumura, C.; Morino, Y. *J. Chem. Phys.* **1986**, *84*, 4205.
- (13) Craig, N. C.; Chen, A.; Suh, K. H.; Klee, S.; Mellau, G. C.; Winnewisser, B. P.; Winnewisser, M. *J. Phys. Chem. A* **1997**, *101*, 9302.
- (14) Stone, S. C.; Philips, L. A.; Fraser, G. T.; Lovas, F. J.; Xu, L.-H.; Sharpe, S. W. *J. Mol. Spectrosc.* **1998**, *192*, 75.
- (15) Brown, D. E.; Beagley, B. *J. Mol. Struct.* **1977**, *38*, 167.
- (16) Craig, N. C.; Chuang, J. I.; Nwofor, C. C.; Oertel, C. M. *J. Phys. Chem. A* **2000**, in press.
- (17) Suenram, R. D.; Grabow, J.-U.; Zuban, A.; Leonov, I. *Rev. Sci. Instrum.* **1999**, *70*, 2127.
- (18) Suenram, R. D.; Lovas, F. J.; Pereyra, W.; Fraser, G. T.; Hight Walker, A. R. *J. Mol. Spectrosc.* **1997**, *181*, 67.
- (19) During the course of these experiments certain products were used, but their use should not be construed as an endorsement by NIST in any way.
- (20) Reinhartz, J. M. L. J.; Dymanus, A. *Chem. Phys. Lett.* **1974**, *24*, 346.
- (21) Ruoff, R. S.; Klotts, T. D.; Emilsson, T.; Gutowsky, H. S. *J. Chem. Phys.* **1990**, *70*, 3142.
- (22) Fraser, G. T.; Suenram, R. D.; Lugez, C. L. *J. Phys. Chem. B* **2000**, *104*, 1141.
- (23) Mukhtarov, J. R.; Kuliev, V. R. *Izv. Akad. Nauk Az. SSSR, Ser. Fiz.-Tekh. Mat. Nauk* **1970**, 132.
- (24) Gordy, W.; Cook, R. L. *Microwave Molecular Spectra, Techniques of Chemistry*, Vol. XVIII, 3rd ed.; John Wiley and Sons: New York, 1984; pp 661, 666.